Flow-regulated endothelial S1P receptor-1 signaling sustains vascular development

Bongnam Jung[1,$], **Hideru Obinata**[1,$], **Sylvain Galvani**[1], **Karen Mendelson**[1,2], **Bisen Ding**[3], **Athanasia Skoura**[4], **Bernd Kinzel**[5], **Volker Brinkmann**[5], **Shahin Rafii**[3], **Todd Evans**[2], and **Timothy Hla**[1,*]

[1]Center for Vascular Biology, Department of Pathology and Laboratory Medicine, Weill Cornell Medical College, Cornell University, New York, NY [2]Department of Surgery, Weill Cornell Medical College, Cornell University, New York, NY [3]Department of Genetic Medicine and Ansary Stem Cell Center, Weill Cornell Medical College, Cornell University, New York, NY [4]Pfizer Inc., Cambridge, MA [5]Novartis Institutes for Biomedical Research, Basel, Switzerland

SUMMARY

During angiogenesis, nascent vascular sprouts fuse to form vascular networks enabling efficient circulation. Mechanisms that stabilize the vascular plexus are not well understood. Sphingosine 1-phosphate (S1P) is a blood-borne lipid mediator implicated in the regulation of vascular and immune systems. Here we describe a mechanism by which the G protein-coupled S1P receptor-1 ($S1P_1$) stabilizes the primary vascular network. A gradient of $S1P_1$ expression from the mature regions of the vascular network to the growing vascular front was observed. In the absence of endothelial $S1P_1$, adherens junctions are destabilized, barrier function is breached, and flow is perturbed resulting in abnormal vascular hypersprouting. Interestingly, $S1P_1$ responds to S1P as well as laminar shear stress to transduce flow-mediated signaling in endothelial cells both *in vitro* and *in vivo.* These data demonstrate that blood flow and circulating S1P activate endothelial $S1P_1$ to stabilize blood vessels in development and homeostasis.

INTRODUCTION

Angiogenesis, the formation of new blood vessels from preexisting vasculature, is a fundamental event in embryonic development, physiological processes, organ regeneration and diseases(Carmeliet and Jain, 2011). The multifunctional endothelial cells (ECs) initiate, sustain and terminate angiogenesis under a variety of physiological and pathological conditions(Butler et al., 2010; Gaengel et al., 2009).

Extravascular expression and paracrine activation of ECs by the vascular endothelial growth factor (VEGF) is a major initiating event in angiogenesis(Ferrara, 2009). The primary stimulus for the extravascular expression of VEGF is hypoxia; reduced oxygen tension signals via the prolyl hydroxylase enzymes to regulate the abundance of hypoxia-inducible

transcription factors which directly induce VEGF expression(Fraisl et al., 2009). VEGF activation of its receptors on the endothelium (VEGFR-2 and VEGFR-3) results in the formation of morphologically distinct tip cells(Gerhardt and Betsholtz, 2005). It was recently shown that VEGFR-2 induction of the Notch ligand Dll4 inhibits tip cell formation by activating the Notch1 receptor in the neighboring cells, thereby suppressing tip cell formation(Hellstrom et al., 2007; Suchting et al., 2007). Concomitantly, stalk cells, which trail behind tip cells, proliferate and differentiate into lumen-containing nascent vascular sprouts(Kamei et al., 2006; Zeeb et al., 2010), and fuse into a primary vascular loop, which is a key step in the initiation of blood flow(Fantin et al., 2010).

Although blood flow is important for blood vessel differentiation, cessation of hypersprouting, remodeling and homeostasis, molecular mechanisms by which ECs sense biomechanical shear forces are poorly understood(Hahn and Schwartz, 2009). *In vitro* studies have identified a signaling complex containing VE-cadherin, PECAM-1 and VEGFR-2 which was required for the transduction of biomechanical forces to cytoskeleton realignment and NF-κB activation in ECs(Tzima et al., 2005). A recent study identified flow-induced miR-126 as a critical factor in aortic arch sprouting angiogenesis in zebrafish(Nicoli et al., 2010). Further, using a microfluidic device, it was proposed that fluid shear forces inhibit EC sprouting induced by positive VEGF gradients *in vitro*(Song and Munn, 2011). Importantly, the relationship of flow-mediated biomechanical signals with angiogenic factor signaling *in vivo* is not clear.

In addition to physiological processes such as embryonic development, organ growth and wound healing, angiogenesis is critical for various diseases such as cancer, age-related macular degeneration (AMD), rheumatoid arthritis and psoriasis. Thus, intensive efforts have been made to develop new anti-angiogenic therapeutics. Indeed, an antibody against VEGF was approved for therapy in metastatic cancers and in AMD(Carmeliet and Jain, 2011; Ferrara, 2009). Better understanding of major mechanisms of angiogenesis may eventually lead to the development of more effective anti-angiogenic therapies.

Sphingosine 1-phosphate (S1P), a bioactive lysophospholipid, is highly enriched in plasma by binding to ApoM in the HDL particle(Christoffersen et al., 2011). Its prototypic receptor $S1P_1$ is induced in angiogenic ECs(Hla et al., 2001; Lee et al., 1998) and is essential for vascular development(Liu et al., 2000). S1P effects on various aspects of vascular function, such as vascular permeability(Sanchez et al., 2003), cell migration(Paik et al., 2001), cell-cell adhesion(Lee et al., 1999), survival(Lee et al., 1998), and tumor angiogenesis(Chae et al., 2004). However, the role of S1P in physiological angiogenesis has not been characterized in the postnatal period. Importantly, the relationship of S1P signaling with primary angiogenic factors, such as VEGF and Notch, and its role in biomechanical signaling is completely unknown.

Here we developed inducible genetic loss-of-function (LOF) and gain-of-function (GOF) models to investigate the role of $S1P_1$ in postnatal angiogenesis. We demonstrate that $S1P_1$ is essential for stabilization of flow-competent neovessel network, and in its absence, breach of vascular barrier function, tissue hypoxia and abnormal vascular patterning ensue. The requirement for $S1P_1$ in vascular network stability is important for normal vascular development and homeostasis. Notably, $S1P_1$ not only responds to the lysophospholipid S1P but also is critical for EC mechanotransduction. These findings provide a mechanistic basis for intravascular, flow-dependent vascular stabilization of the primary vascular network.

RESULTS

Genetic ablation of murine *S1pr1* results in abnormal retinal vasculature

We developed a global and inducible gene deletion model for *S1pr1* in the mouse (*S1pr1^f/f Rosa26-Cre-ER^T2*; referred to as *S1p1 KO*). When *S1p1 KO* mice were given Tamoxifen from postnatal day 1 (P1) to P3, efficient and specific gene deletion was observed in the retina at P4 and thereafter (Figures S1A and S1B). Analysis of the retina indicated a profound alteration in vascular phenotype in *S1p1 KO* mice. Expansion of the primary vascular plexus was severely affected resulting in abnormal vascular patterning (Figures 1A and 1B). Specifically, increased number of filopodia-containing tip cells, branch points, and dilated vessels were observed (Figures 1C–1H).

To determine whether cell proliferation is responsible, we performed BrdU incorporation assay using *S1p1 KO* animals and their littermate controls. Staining for BrdU followed by lectin was carried out to visualize proliferating retinal ECs (Figures S1C–S1F). Although there is no apparent difference in total BrdU$^+$ cell numbers, EC proliferation (BrdU$^+$Lectin$^+$) in *S1p1 KO* mouse retinas was increased. Thus, reduced vascularization in the *S1p1 KO* mouse retinas was not caused by a deficiency in EC proliferation.

S1pr1-deleted mice die at embryonic day 10.5–12.5, which is associated with defective vascular maturation, extensive hemorrhage and edema(Allende et al., 2003; Liu et al., 2000). Further mechanistic studies also indicated the role of S1P$_1$ in the regulation of EC/pericyte interactions(Paik et al., 2004). Thus, we examined whether mural cell recruitment was altered during different stages of the retinal vasculature development. Interestingly, smooth muscle actin (SMA)$^+$ vascular smooth muscle cells in arterioles (Figure S1G), or NG2$^+$ pericytes in capillaries (Figure S1H) were indistinguishable between WT and *S1p1 KO* retinal vessels. These results suggest that the vascular endothelial alterations observed in the *S1p1 KO* mice was a primary effect and not secondary to a defect in mural cell recruitment.

EC-intrinsic S1P$_1$ signaling regulates vascular patterning

We next investigated whether EC-intrinsic S1P$_1$ regulates vascular development in the retina. We developed EC-specific inducible knockout mice (*S1pr1^f/f VE-cadherin-Cre-ER^T2*; referred to as *S1p1 ECKO*) to address this question. qRT-PCR analysis using ECs isolated from the lung tissue in WT and *S1p1 ECKO* animals shows efficient *S1pr1* gene deletion. Compensatory changes in the expression of S1P$_2$ and S1P$_3$ receptors were not observed (data not shown). Similarly, *S1p1 ECKO* animals exhibited abnormal vascular phenotype characterized by defective vascularization, hypersprouting, increased branching, and dilated morphology (Figures 1I–1P). These results strongly suggest EC-autonomous function of S1P$_1$ in the regulation of retinal vascular development. We also examined mural cell recruitment in *S1p1 ECKO* at different developmental stages as well as different regions of the retinal vasculature. Mural cell coverage of the retinal vessels in *S1p1 ECKO* animals was comparable to WT counterparts (Figures S1G–S1H).

The vascular phenotype of S1P$_1$ LOF is similar to the attenuated Notch signaling observed in the *Dll4^+/−* mutant retinas(Hellstrom et al., 2007; Suchting et al., 2007), raising the possibility that S1P$_1$ and Notch signaling pathways are epistatic in the regulation of angiogenesis. However, Notch target genes were not altered significantly in the retinal tissue of inducible *S1p1 KO* mice (Figure S2A). Treatment of human umbilical vein endothelial cells (HUVEC) with S1P to activate the S1P$_1$ receptor also did not change the expression of Notch target genes (data not shown). These data suggest that Notch is not a downstream target of S1P$_1$ in ECs. Additionally, treatment of HUVEC with Dll4 polypeptide coated on a solid surface promoted strong induction of *Hes1* mRNA expression, while no alteration on S1P$_1$ mRNA expression was observed (Figure S2B), indicating that S1P$_1$ is not downstream

of Dll4/Notch pathway. Together, these experiments suggest that $S1P_1$ signaling pathway is likely parallel to Notch signaling in neovessel formation.

Overexpression of $S1P_1$ suppresses endothelial sprouting

Given these findings, we hypothesized that overexpression of $S1P_1$ might suppress tip cell formation and hypersprouting in retinal vasculature. To address this, we examined the inducible overexpression of $S1P_1$ in a transgenic mouse system ($S1pr1^{f/stop/f} Rosa26-Cre-ER^{T2}$; referred to as *S1p1 GOF*) (Figure S1I). Cre-mediated selective $S1P_1$ gene activation was confirmed by PCR as shown in Figure S1J. Remarkably, overexpression of $S1P_1$ induced a sparse vascular network at mid region and fewer tip cells at the vascular leading front (Figures 2A–2F). Quantitative morphometry confirmed reduced tip cells (Figure 2G), reduced branch points (Figure 2H), and dilated vasculature (Figure 2I) in *S1p1 GOF* retinas. Further, mural cell coverage by SMA$^+$ cells as well as NG2$^+$ cells in *S1p1 GOF* were similar to WT counterparts, shown in Figures S1G–S1H.

Gradient of $S1P_1$ expression in the retinal vasculature

We next examined the expression pattern of $S1P_1$ in retinal vasculature using the *S1pr1*$^{LacZ/+}$ mouse(Liu et al., 2000). *S1pr1* expression was increased from the leading front (low) to the mature, flow-positive regions (high) of the vascular network (Figures 3A and 3B). X-gal staining was co-localized with an EC marker, PECAM-1 or lectin (Figures 3C–3G). In contrast, GFAP-(astrocyte marker) and NG2-(pan-pericyte marker) positive cells were devoid of X-gal staining (Figures 3H and 3I), indicating the restricted expression of *S1pr1* in endothelium. Moreover, the graded expression pattern of *S1pr1* was correlated with receptor protein expression, as determined by immunofluorescence confocal microscopy (Figure S3).

Dysregulated blood flow and leakage in $S1P_1$-null vessels *in vivo*

S1P activation of its receptors in ECs, particularly $S1P_1$ and $S1P_3$, results in activation of Rac and Rho GTPases and coordinated cytoskeletal changes which are obligate steps in the assembly of VE-cadherin-mediated adherens junctions(Lee et al., 1999). Since proper assembly of the adherens junctions and subsequent signal transduction events are essential for maintenance of the EC morphogenesis and functionality(Montero-Balaguer et al., 2009), *S1p1 ECKO* mice were analyzed for blood flow and permeability by intra-cardiac injection of high molecular weight FITC-dextran (to indicate vascular leakage) and isolectin B4 (to indicate vascular perfusion). Strikingly, the vessels of the *S1p1 ECKO* retina displayed poor isolectin B4 labeling compared to the WT counterparts (Figures 4A, 4D, 4G and 4J), suggesting that $S1P_1$ is critical for proper perfusion of blood vessels. Further, *S1p1 ECKO* retinas showed extravascular FITC-dextran, indicating enhanced vascular leakage (Figures 4B, 4E, 4H and 4K). These results suggest suboptimal blood flow and breach of barrier function of the vessels in the absence of $S1P_1$.

To further confirm the perturbation in blood flow upon $S1P_1$ loss, we examined oxygenation of the retinal tissue in *S1p1 ECKO* mice with oxygen-sensitive compound hypoxyprobe-1(Chen et al., 2009). As shown in Figures 4M–4R, vascularized areas of the *S1p1 ECKO* retina were severely hypoxic compared to the WT counterparts. Moreover, VEGF-A polypeptide expression was significantly elevated in the *S1p1 ECKO* retinas but not in plasma (Figures S4A and S4B). These results suggest that loss of $S1P_1$ results in reduced blood flow, which induces local tissue hypoxia and VEGF-A expression.

Increased VEGF-A expression in the retina could drive the hypersprouting phenotype observed in the *S1p1 ECKO* retinal vessels. To test this hypothesis, a potent VEGFR-2 inhibitor SU5416 was administered in combination with FTY720, a potent functional

antagonist which induces proteosomal degradation of the $S1P_1$ receptor(Oo et al., 2011). Systemic administration of FTY720 (5 mg/Kg) to newborn mice resulted in increased tip cell numbers, similar to genetic *S1pr1* LOF. Further, FTY720-induced tip cell formation was significantly suppressed by SU5416 treatment (Figures S4C–S4E).

Increased phosphorylation of VE-cadherin, especially at Y^{658} and Y^{731} residues, is known to be associated with junctional destabilization and VEGF signaling (Dejana et al., 2008). We therefore examined the role of $S1P_1$ on phosphorylation state of VE-cadherin *in vivo*. Lung tissue extracts from *S1p1 ECKO* animals exhibited ~ 2-fold increase in phospho-VE-cadherin levels at both Y^{658} and Y^{731} (Figure 4S), indicating junctional destabilization. We also examined the proteolytic sensitivity of VE-Cadherin by trypsin in retina(Gavard and Gutkind, 2006). The rationale of this experiment is that junction-associated VE-cadherin will be more trypsin resistant. In contrast, when adherens junctions are destabilized, VE-cadherin will be more accessible to trypsin cleavage. When retinal tissue was treated with trypsin *ex vivo*, *S1p1 ECKO* showed greater sensitivity to protease cleavage than the WT counterparts, whereas other membrane proteins such as N-cadherin, podocalyxin, VEGFR-2 and PECAM-1 did not show differential trypsin sensitivity (Figure 4T), suggesting junctional destabilization in *S1p1 ECKO*.

$S1P_1$ is essential for fluid shear stress signaling in ECs

Flow-dependent fluid shear forces activate the endothelial mechanosensing machinery and trigger intracellular signals such as heterotrimeric G protein activation, small GTPase Rac activation, ERK and Akt phosphorylation, eNOS activation and VE-cadherin junction assembly(Hahn and Schwartz, 2009). Since $S1P_1$ and laminar shear force signals are largely overlapping, we tested if $S1P_1$ receptor itself is required for EC shear stress signaling *in vitro*. Antagonism of $S1P_1$ with FTY720-P completely blocked shear stress-induced adherens junction assembly (Figures 5A–5D), as well as phosphorylation of ERK, Akt, and eNOS (Figure 5E) in HUVEC. Similarly, shRNA-mediated downregulation of $S1P_1$ also inhibited shear stress-induced ERK activation (Figure 5F). Further, overexpression of $S1P_1$ by adenovirus restored shear stress-induced ERK activation in ECs in which $S1P_1$ was inhibited by FTY720-P (Figure 5G). In addition to such acute signaling events, chronic application of laminar shear stress induces alignment of EC monolayers to the direction of flow and elongation of cell shape(Noria et al., 1999) as well as planar polarity of intracellular organelles such as the microtubule organizing center and the Golgi apparatus(Tzima et al., 2003). When $S1P_1$ was downregulated by either shRNA or FTY720-P treatment, shear-induced EC alignment was significantly suppressed (Figures 5I–5L). Polarized localization of eNOS in the perinuclear/Golgi region(Sessa et al., 1995) in the direction of flow was abolished by FTY720-P treatment (Figure S5A). Remarkably, re-expression of $S1P_1$ restored EC alignment to the direction of flow (Figures 5M and 5O). These data suggest that $S1P_1$ is necessary for both acute and chronic signaling events induced by laminar shear stress in ECs.

The requirement for $S1P_1$ in laminar shear stress signaling may simply reflect the secretion of S1P(Venkataraman et al., 2008) followed by export and activation of $S1P_1$. However, neither pharmacologic inhibition of sphingosine kinases nor shRNA-mediated knockdown of endothelial S1P transporter Spns2(Kawahara et al., 2009) had an effect on laminar shear stress-induced ERK phosphorylation(Figures S5B–S5D), raising the possibility that $S1P_1$ can be activated in a ligand-independent manner in response to laminar shear stress. To address this hypothesis, we utilized a $S1P_1$ mutant (R120A), which is deficient in S1P binding(Wang et al., 2001). This residue docks the phosphate moiety of the S1P and thus is essential for ligand activation of the receptor (Wang et al., 2001; Hanson et al., 2012). We also used the C-terminal phosphorylation-deficient mutant ($S1P_1$S5A) which is defective in agonist-activated endocytosis, and therefore exhibit increased plasma membrane

residency(Oo et al., 2007). As expected, the $S1P_1R120A$ mutant did not respond to S1P or FTY720-P in ERK activation or internalization experiments (Figures S5E and S5F). $S1P_1S5A$ mutant still responded to S1P in the ERK phosphorylation assay, but exhibited defective endocytosis even after FTY720-P treatment (Figure S5F). In HUVEC, both $S1P_1R120A$ and $S1P_1S5A$ mutants restored shear stress-induced ERK activation when $S1P_1$ was antagonized by FTY720-P (Figure 5H). Interestingly, the $S1P_1R120A$ mutant allowed laminar shear stress-mediated EC alignment (Figures 5N, 5O **and** S5A), and polarized alignment of the Golgi apparatus (eNOS) (Figure S5A). suggesting that $S1P_1$ receptor itself, in a ligand-independent manner, plays an essential role in EC shear stress signaling.

Flow-dependent $S1P_1$ signaling *in vivo* in vascular homeostasis

To examine the relationship between $S1P_1$ and flow-dependent EC function *in vivo*, we analyzed the linear part of the aorta (descending aorta) which is subject to steady laminar shear stress(Davies, 2009). $S1P_1$ expression was observed on the plasma membrane co-localized with VE-cadherin. In contrast, in areas of turbulent shear, i.e. the lesser curvature of the aorta, $S1P_1$ presence at the adherens junctions is lost and $S1P_1$ is found intracellularly in the endocytotic vesicles as indicated by strong co-localization with EEA-1 (Figures 6A–6D).

In *S1p1 ECKO,* significantly reduced phospho-eNOS staining was observed in the descending aorta (Figures 6E–6J), suggesting that $S1P_1$ mediates eNOS activation *in vivo.* In agreement with the results from the aortic vasculature, phosphorylation of eNOS was significantly reduced in *S1p1 ECKO* retinas, shown in Figures 6K and 6L. Interestingly, cellular and nuclear morphology in the descending aorta from *S1p1 ECKO* mice showed significant alterations. Specifically, ECs (both cytoplasm and nucleus) from *S1p1 ECKO* mice were round, less aligned/elongated (Figures 6M and 6N). These data provide strong *in vivo* evidence that $S1P_1$ is an essential component of flow-dependent biomechanical signaling in the endothelium.

DISCUSSION

The main finding of this work is that $S1P_1$ signaling in ECs regulates sprouting angiogenesis. Lack of $S1P_1$ promoted hypersprouting whereas overexpression of $S1P_1$ suppressed sprouting angiogenesis in the developing retinal vasculature. Since tip/stalk cell specification is a key event in subsequent vascular patterning events, i.e., hierarchical branching and vascular network architecture, the entire vascular network morphology is critically dependent on precise signaling of $S1P_1$.

Interestingly, $S1P_1$ expression is strongly induced in the mature, flow-positive regions of the vascular network. In sharp contrast, the sprouting vascular front, the tip and stalk cell region, expressed very low levels of *S1pr1*. The induction of $S1P_1$ could be due to the action of flow-regulated transcription factors such as KLF2. Indeed, in lymphocytes, KLF2 is required for $S1P_1$ expression(Carlson et al., 2006). We also show that the induction of $S1P_1$ is associated with cessation of EC sprouting. The effect is EC intrinsic and occurred prior to the recruitment of mural cells. These findings reveal a previously unappreciated function of $S1P_1$ to suppress ectopic sprouting driven by extrinsic VEGF signaling from outside the vasculature. Even though the precise mechanism by which $S1P_1$ inhibits ectopic sprouting merits further investigation, our results suggest crosstalk between $S1P_1$ and VEGFR-2 signaling pathways during sprouting angiogenesis. Namely, lack of $S1P_1$ results in the local tissue hypoxia and enhanced VEGF-A production, leading to increased EC proliferation and sprouting. Further, blockade of VEGFR-2 signaling partially reverses FTY720-induced vascular hypersprouting. The ability of $S1P_1$ receptor to regulate vascular hypersprouting may have implications in physiology and pathology. For example, exaggerated VEGF

signaling in pathological conditions such as tumor angiogenesis, AMD and rheumatoid arthritis could be potentially controlled by activating EC $S1P_1$ signaling.

Secondly, we found that the ability of $S1P_1$ to regulate sprouting angiogenesis was independent of Notch signaling. Even though attenuated Notch signaling by hypomorphic Dll4 gene function produces a similar phenotype as the $S1P_1$ LOF, analysis of both *in vivo* and *in vitro* systems suggests that $S1P_1$ effect occurs independently of Notch signaling. Further, recent findings suggest that Dll4/Notch signaling can be independent of VEGFR-2 signaling during angiogenic sprouting (Benedito et al., 2012). Given the differential, and dynamic expression pattern of Notch ligands (i.e. Dll4 and Jagged-1) and its relationship to VEGFR-2 and VEGFR-3, versus flow-dependent, gradient of $S1P_1$ expression during vessel development, it is likely that $S1P_1$ and Notch signaling systems regulate different aspects of the angiogenic process: Notch/Dll4/Jagged-1 controls tip/stalk cell transition of the ECs whereas $S1P_1$ receptor signaling regulates the stability of the primary vascular network.

Our studies demonstrate that $S1P_1$ function is required for adherens junction stability in the developing retinal vasculature. Lack of $S1P_1$ promoted junctional destabilization, as evidenced by increased tyrosine phosphorylation, trypsin sensitivity of the extracellular domain of VE-cadherin and increased permeability of intravascular dextran from vessels. This occurs concomitantly with reduced capillary perfusion and tissue hypoxia. It is likely that such changes induce local production of VEGF-A, which was significantly increased in retinal tissue extracts. Since the $S1P_1$ LOF-induced hypersprouting response is sensitive to VEGFR-2 inhibition, we suggest that exaggerated VEGF signaling is critical. Thus, we propose that $S1P_1$ indirectly limits VEGF signaling in angiogenesis by regulating junction- and flow-dependent mechanisms. However, we cannot exclude the possibility that $S1P_1$ acts upstream of VEGF and that VEGF acts as an intermediary of $S1P_1$ effects on flow responses and junctional stabilization. These possibilities need to be addressed in relevant *in vivo* systems.

Surprisingly, $S1P_1$-null vessels did not exhibit any pericyte recruitment defect in capillaries as well as vascular smooth muscle cell investment in arteries and veins, in contrast to the pericyte recruitment defect in the dorsal aorta of the mouse embryos(Liu et al., 2000). However, breach of the EC barrier function, reduced flow and tissue hypoxia were prominent when $S1P_1$ was ablated in an EC-specific manner. Although we cannot completely rule out the possibility that EC $S1P_1$ might control the strength of the interaction between ECs and mural cells, our findings suggest that the ability of $S1P_1$ to regulate pericyte recruitment might be tissue-specific or stage-specific.

Another key finding of this work is that $S1P_1$ is an essential component of fluid shear stress sensing. *In vitro*, $S1P_1$ is required for ECs to sense fluid shear stress and transduce intracellular signals such as ERK1/2 and Akt phosphorylation as well as cell alignment to the direction of flow. Indeed, downstream of Akt, critical EC regulators such as eNOS are activated. Furthermore, $S1P_1$R120A mutant, which does not bind S1P, can still induce shear-mediated responses. Thus $S1P_1$, which is induced in the flow-positive vascular networks, responds not only to blood-derived S1P but also to biomechanical signals and transduces intracellular events that promote vascular homeostasis and stability of the nascent vascular network.

Our data also show that the subcellular localization of $S1P_1$ in the aortic endothelium *in vivo* is regulated by flow. In the descending aorta where the endothelium is constantly subject to steady laminar shear stress, $S1P_1$ is localized on the plasma membrane whereas in the lesser curvature where the endothelium is exposed to turbulent shear stress, $S1P_1$ appears to be intracellular. Previous studies have shown that irreversible internalization of $S1P_1$ is

associated with ubiquitination and degradation(Oo et al., 2007). Therefore, abnormal shear signaling may induce a $S1P_1$ hypomorphic state in ECs. Indeed, our data demonstrate that $S1P_1$ function in the endothelium *in vivo* is necessary to maintain the activity of the eNOS enzyme, supporting the notion that fluid shear stress signaling *in vivo* requires $S1P_1$.

Previous work has attempted to define the molecular details of the shear stress sensor in EC. Although molecular identity of the primary sensor has remained elusive, a protein complex composed of VE-cadherin, VEGFR-2 and PECAM-1 was shown to be critical for fluid shear stress-induced EC alignment(Tzima et al., 2005). Further, Tzima et al. showed that this complex was crucial for fluid shear-mediated phosphorylation of Akt, Src, and VE-cadherin itself. In addition, other studies have implicated the critical role of integrins, G proteins and plasma membrane domains in shear stress signaling(Hahn and Schwartz, 2009). The *in vivo* demonstration that $S1P_1$ regulates phosphorylation and protease sensitivity of VE-cadherin suggests a critical mechanism in flow-mediated vascular stabilization. Therefore, a scenario which merits further investigation is that the shear sensing complex composition is regulated by $S1P_1$ signaling. Alternatively, $S1P_1$ intrinsically could have a force-sensing domain or can be associated with another molecule capable of sensing biomechanical forces on the cell surface. In that context, the association of $S1P_1$ with the lymphocyte activation antigen CD69 in immune cells, and ligand-independent activation of $S1P_1$ by CD69 has been described(Bankovich et al., 2010; Shiow et al., 2006). In fact, CD69-induced down-regulation of $S1P_1$ is a key event in lymphocyte retention in secondary lymphoid organs. Our finding that $S1P_1$ signaling is critical for ECs to sense biomechanical forces in a S1P-independent manner suggests the existence of a mechanosensitive co-receptor for $S1P_1$ in the vascular endothelium.

Another interesting finding from this study is that lack of $S1P_1$ perturbed physiological flow in the developing retinal vascular network. This could be due to decreased activation of eNOS and reduced production of NO, a potent vasodilator. Further, disrupted barrier function of the endothelium could also contribute to poor blood flow. Additionally, NO-dependent signaling pathways have been implicated in the regulation of adherens junctions in the endothelium (Thibeault et al., 2010).

In summary, this study has revealed several mechanistic insights in the process of angiogenesis. Plasma-derived S1P and blood flow transduce signals via $S1P_1$ in ECs to promote primary vascular network stability and suppress ectopic sprout formation. We propose that this is a general mechanism by which blood vessels use both extravascular signals such as VEGF and intravascular signals including S1P and flow to achieve a stable primary vascular plexus formation. Accordingly, we show that the growing vascular network contains $S1P_1$ as an integral component of the flow-sensing machinery and subsequent signaling events are important for vascular stability and physiological blood flow. This intravascular signaling paradigm, which appears to be required during development and homeostasis, maybe dysregulated in vascular diseases associated with inflammatory and neoplastic conditions.

EXPERIMENTAL PROCEDURES

Animals

All animal experiments were approved by the Weill Cornell Institutional Animal Care and Use Committee. *S1pr1^{LacZ/+}* (Liu et al., 2000) and *S1pr1^{f/f}* (Allende et al., 2003) mice were provided by Dr. Richard Proia (NIDDK, NIH). *S1pr1^{f/f}* mice are crossed to *Rosa26-Cre-ER^{T2}* (a gift from Dr. Guo-Hua Fong, University Connecticut Health Center)(Ghosh et al., 2009) or to *VE-Cadherin-Cre-ER^{T2}* (a gift from Dr. Ralf Adams, Max Planck Institute, Muenster, Germany)(Pitulescu et al., 2010) to generate *S1pr1^{f/f} Rosa26-Cre-ER^{T2}*, and

$S1pr1^{f/f}$ VE-Cadherin-Cre-ER^{T2} mice, respectively. $S1p1^{f/stop/f}$ was generated by knocking in the transgene into ES cells, and crossed to Rosa26-Cre-ER^{T2} to yield $S1p1^{f/stop/f}$ Rosa26-Cre-ER^{T2} animals. Littermates from $S1pr1^{f/f}$ ±Rosa26-Cre-ER^{T2}, $S1pr1^{f/f}$ ±VE-Cadherin-Cre-ER^{T2} or $S1p1^{f/stop/f}$ ±Rosa26-Cre-ER^{T2} animals were fed Tamoxifen (150 μg p.o.) for 3 days from postnatal day 1 (P1) to P3. Genotyping was done by PCR using tail biopsies or by quantitative real-time PCR using RNA isolated from retinal tissues. Mouse pups at P4 or P5 were examined for retinal vascular development as described previously(Hellstrom et al., 2007; Skoura et al., 2007).

Tissue Whole Mount Preparation Immunofluorescence Staining, and Imaging

Retinal dissection and immunofluorescence staining was performed as previously described(Gerhardt et al., 2003; Skoura et al., 2007). Briefly, retinal tissues were fixed in 4 % PFA in PBS at 4°C. Retinas were permeabilized in PBS with 1 % BSA, 0.5 % Triton X-100 at room temperature (RT) for 30 min, followed by washing in PBlec buffer (PBS (pH 6.8), 1 % Triton X-100, 0.1 mM $CaCl_2$, 0.1 mM $MgCl_2$, 0.1 mM $MnCl_2$). For aortic dissection, blood was removed by perfusion with PBS and 4 % PFA. The aortic tree was carefully removed from the heart to the renal aorta and postfixed for 20 min in 4 % PFA, and greater curvature and descending aortas were isolated. After quenching using 100 mM glycine (pH 7.4), tissues were permeabilized, washed, and blocked with PBS containing 2 % FCS, 1 % BSA, 75 mM NaCl, 18 mM $Na_3C_6H_5O_7$, and 0.05 % Triton X-100 for 2 hrs at RT(Filipe et al., 2008). Standard protocols and commercially available antibodies were used for the whole mount retinal- or en face aortic tissue immunostaining. Confocal immuofluorescence images of the tissues were captured on a Olympus Fluoview confocal microscope.

X-gal Staining

X-gal staining was performed to visualize the expression of S1pr1 in the retina as previously described(Liu et al., 2000). In brief, the eyes were enucleated from P4 pups from $S1p1^{LacZ/+}$ or littermate control, fixed in 4 % PFA for 10 min at RT, and post-fixed in 2 % formaldehyde/2 % glutaraldehyde in PBS for 1 hr on ice. After washing in PBS, retinas were incubated in PBS containing 1 mg/ml of X-gal in 5 mM $K_3Fe(CN)_6$, and 2 mM $MgCl_2$ at 37 °C until the color was developed. To define S1pr1-expressing cell types, X-gal-stained retinas were further processed for PECAM-1 (endothelial cells), GFAP (astrocytes) or NG2 (pericytes) staining in PBlec buffer (Stenzel et al., 2011).

Assessment of Endothelial Barrier Function by Intracardiac FITC-dextran Injection

High-molecular weight FITC-dextran injection was performed to visualize lumen formation of the retina as described previously(Gerhardt et al., 2003) in combination with lectin injection to assess functional vessels/blood flow. Briefly, FITC-dextran (2000 kDa, Sigma Aldrich, FD2000S) and Alexa-conjugated lectin (Griffonia simplicifolia GS-IB$_4$ lectin) were prepared in PBS at the concentration of 25 mg/ml, and 1 μg/ml, respectively. P5 S1p1 ECKO and littermate control were given anesthesia, and intracardiac injection of FITC-dextran and lectin solution was performed. After 3 min, the eyes were enucleated, fixed in 4 % PFA, and retinal tissue was processed for VE-Cadherin staining and confocal immunofluorescence microscopy.

Retinal Hypoxia Staining

To determine the hypoxic area of the retinal vasculature, P5 pups were subjected to intraperitoneal injection of the oxygen-sensitive compound Hypoxyprobe-1 (pimonidazole hydrochloride, Hypoxyprobe, Inc) at a dosage of 60 mg/Kg body weight. After 90 min, the

retinas were fixed in 4% PFA, dissected, permeabilized, and stained with FITC-conjugated anti-Hypoxyprobe-1 antibody followed by lectin to visualize vessels(Chen et al., 2009).

Ex vivo Trypsin Sensitivity Assay

VE-cadherin sensitivity to the trypsin protease in retinal tissue was adapted as described(Gavard and Gutkind, 2006). Eyeballs from P5 animals were enucleated, and the retina was exposed by removal of cornea, anterior/posterior chambers, lens and hyaloid. The eyecup was incubated with trypsin/EDTA-containing HBSS (0.05 % Trypsin, 20 mM glucose supplement) or HBSS (-Trypsin, 20 mM glucose supplement). After 1 hr incubation at 37°C, tissue was rinsed three times in FBS-containing medium to inactivate trypsin, retina was dissected out and lysed in RIPA buffer for western blot analysis.

Fluid Shear Stress Assay

For short-term shear application (up to 1 hr), human umbilical vein endothelial cells (HUVEC) were cultured to confluence on fibronectin-coated glass slides, and starved for 3 hr in the medium containing 1 % charcoal-stripped FCS, 20 mM HEPES (pH 7.4) and antibiotics, then subjected to fluid shear stress at 8 dyne/cm^2 in a parallel flow chamber as described before(Venkataraman et al., 2008; Wadhwa et al., 2002). For long-term shear application (12 hr), HUVEC were subjected to fluid shear stress at 10 dyne/cm^2 using BioFlux200 system (Fluxion) according to the manufacturer's instruction in the normal growth medium supplemented with 20 mM HEPES. Where indicated, wild-type human $S1P_1$, R120A(Wang et al., 2001) and S5A(Oo et al., 2007) mutants of human $S1P_1$ were overexpressed by lentiviral transduction, and suppression of endogenous $S1P_1$ were achieved either by treating the cells with FTY720-P for 3 h or by transducing shRNA (The RNAi Consortium clone TRCN0000011362, Sigma-Aldrich) in a lentiviral vector. The alignment of the cells after 12 hr shear application was evaluated by visualizing VE-cadherin, actin stress-fibers, eNOS and nuclei.

Western blot analysis

HUVEC or tissues were lysed in RIPA buffer (50 mM Tris (pH 7.4), 150 mM NaCl, 1 mM EDTA, 0.5 % Triton X-100, and 0.5 % Sodium deoxycholate) containing phosphatase inhibitors (1 mM Na_3SO_4, 1 mM NaF, and 5 mM β-glycerophosphate) and 1×protease inhibitors (Calbiochem). Protein concentration was determined by Bio-Rad assay (Bio-Rad protein dye reagent, Bio-Rad), and equal amount of proteins were loaded onto NUPAGE Novex 4–12 % Bis-Tris gel (Invitrogen). Transferred proteins onto nitrocellulose membrane were probed with the antibody against total and phosphorylated ERK, Akt, eNOS, and VE-cadherin, or EC markers. Detailed information for antibodies used is described on Supplementary Experimental Procedures.

Quantitative Analysis

Quantification for retinal vascularization and sprouting angiogenesis was carried out as previously described(Hellstrom et al., 2007; Skoura et al., 2007). Percentage of the vascularized area over total area was analyzed using Image J software (National Institutes of Health). At least three animals were used for the analysis of each time point or treatment unless otherwise indicated. Quantification for shear-mediated EC alignment was performed by scoring the cells as 'aligned' when the longer-axis of the cell was more than 2 fold of the shorter-axis in length, and the longer-axis was within +/− 15 degree against the direction of flow. More than 400 cells per treatment in 4 independent experiments were calculated using Image J software.

Statistical analysis was carried out by the unpaired Student's *t*-test. The differences were considered statistically significant at *P < 0.05*. Data are shown as mean ± SEM except quantification for the EC alignment (mean ± SD).

Supplementary Material

Refer to Web version on PubMed Central for supplementary material.

Acknowledgments

References

Allende ML, Yamashita T, Proia RL. G-protein-coupled receptor S1P1 acts within endothelial cells to regulate vascular maturation. Blood. 2003; 102:3665–3667. [PubMed: 12869509]

Bankovich AJ, Shiow LR, Cyster JG. CD69 suppresses sphingosine 1-phosophate receptor-1 (S1P1) function through interaction with membrane helix 4. J Biol Chem. 2010; 285:22328–22337. [PubMed: 20463015]

Benedito R, Rocha SF, Woeste M, Zamykal M, Radtke F, Casanovas O, Duarte A, Pytowski B, Adams RH. Notch-dependent VEGFR3 upregulation allows angiogenesis without VEGF-VEGFR2 signalling. Nature. 2012; 484:110–114. [PubMed: 22426001]

Butler JM, Kobayashi H, Rafii S. Instructive role of the vascular niche in promoting tumour growth and tissue repair by angiocrine factors. Nat Rev Cancer. 2010; 10:138–146. [PubMed: 20094048]

Carlson CM, Endrizzi BT, Wu J, Ding X, Weinreich MA, Walsh ER, Wani MA, Lingrel JB, Hogquist KA, Jameson SC. Kruppel-like factor 2 regulates thymocyte and T-cell migration. Nature. 2006; 442:299–302. [PubMed: 16855590]

Carmeliet P, Jain RK. Molecular mechanisms and clinical applications of angiogenesis. Nature. 2011; 473:298–307. [PubMed: 21593862]

Chae SS, Paik JH, Furneaux H, Hla T. Requirement for sphingosine 1-phosphate receptor-1 in tumor angiogenesis demonstrated by in vivo RNA interference. J Clin Invest. 2004; 114:1082–1089. [PubMed: 15489955]

Chen J, Connor KM, Aderman CM, Willett KL, Aspegren OP, Smith LE. Suppression of retinal neovascularization by erythropoietin siRNA in a mouse model of proliferative retinopathy. Invest Ophthalmol Vis Sci. 2009; 50:1329–1335. [PubMed: 18952918]

Christoffersen C, Obinata H, Kumaraswamy SB, Galvani S, Ahnstrom J, Sevvana M, Egerer-Sieber C, Muller YA, Hla T, Nielsen LB, et al. Endothelium-protective sphingosine-1-phosphate provided by HDL-associated apolipoprotein M. Proc Natl Acad Sci U S A. 2011; 108:9613–9618. [PubMed: 21606363]

Davies PF. Hemodynamic shear stress and the endothelium in cardiovascular pathophysiology. Nat Clin Pract Cardiovasc Med. 2009; 6:16–26. [PubMed: 19029993]

Dejana E, Orsenigo F, Lampugnani MG. The role of adherens junctions and VE-cadherin in the control of vascular permeability. J Cell Sci. 2008; 121:2115–2122. [PubMed: 18565824]

Fantin A, Vieira JM, Gestri G, Denti L, Schwarz Q, Prykhozhij S, Peri F, Wilson SW, Ruhrberg C. Tissue macrophages act as cellular chaperones for vascular anastomosis downstream of VEGF-mediated endothelial tip cell induction. Blood. 2010; 116:829–840. [PubMed: 20404134]

Ferrara N. Vascular endothelial growth factor. Arterioscler Thromb Vasc Biol. 2009; 29:789–791. [PubMed: 19164810]

Filipe C, Lam Shang Leen L, Brouchet L, Billon A, Benouaich V, Fontaine V, Gourdy P, Lenfant F, Arnal JF, Gadeau AP, et al. Estradiol accelerates endothelial healing through the retrograde commitment of uninjured endothelium. Am J Physiol Heart Circ Physiol. 2008; 294:H2822–2830. [PubMed: 18441207]

Fraisl P, Mazzone M, Schmidt T, Carmeliet P. Regulation of angiogenesis by oxygen and metabolism. Dev Cell. 2009; 16:167–179. [PubMed: 19217420]

Gaengel K, Genove G, Armulik A, Betsholtz C. Endothelial-mural cell signaling in vascular development and angiogenesis. Arterioscler Thromb Vasc Biol. 2009; 29:630–638. [PubMed: 19164813]

Gavard J, Gutkind JS. VEGF controls endothelial-cell permeability by promoting the beta-arrestin-dependent endocytosis of VE-cadherin. Nat Cell Biol. 2006; 8:1223–1234. [PubMed: 17060906]

Gerhardt H, Betsholtz C. How do endothelial cells orientate? EXS. 2005:3–15. [PubMed: 15617467]

Gerhardt H, Golding M, Fruttiger M, Ruhrberg C, Lundkvist A, Abramsson A, Jeltsch M, Mitchell C, Alitalo K, Shima D, et al. VEGF guides angiogenic sprouting utilizing endothelial tip cell filopodia. Journal of Cell Biology. 2003; 161:1163–1177. [PubMed: 12810700]

Ghosh M, Aguila HL, Michaud J, Ai Y, Wu MT, Hemmes A, Ristimaki A, Guo C, Furneaux H, Hla T. Essential role of the RNA-binding protein HuR in progenitor cell survival in mice. J Clin Invest. 2009; 119:3530–3543. [PubMed: 19884656]

Hahn C, Schwartz MA. Mechanotransduction in vascular physiology and atherogenesis. Nat Rev Mol Cell Biol. 2009; 10:53–62. [PubMed: 19197332]

Hanson MA, Roth CB, Jo E, Griffith MT, Scott FL, Reinhart G, Desale H, Clemons B, Cahalan SM, Schuerer SC, et al. Crystal structure of a lipid G protein-coupled receptor. Science. 2012; 335:851–855. [PubMed: 22344443]

Hellstrom M, Phng LK, Hofmann JJ, Wallgard E, Coultas L, Lindblom P, Alva J, Nilsson AK, Karlsson L, Gaiano N, et al. Dll4 signalling through Notch1 regulates formation of tip cells during angiogenesis. Nature. 2007; 445:776–780. [PubMed: 17259973]

Hla T, Lee MJ, Ancellin N, Paik JH, Kluk MJ. Lysophospholipids--receptor revelations. Science. 2001; 294:1875–1878. [PubMed: 11729304]

Kamei M, Saunders WB, Bayless KJ, Dye L, Davis GE, Weinstein BM. Endothelial tubes assemble from intracellular vacuoles in vivo. Nature. 2006; 442:453–456. [PubMed: 16799567]

Kawahara A, Nishi T, Hisano Y, Fukui H, Yamaguchi A, Mochizuki N. The sphingolipid transporter spns2 functions in migration of zebrafish myocardial precursors. Science. 2009; 323:524–527. [PubMed: 19074308]

Lee MJ, Thangada S, Claffey KP, Ancellin N, Liu CH, Kluk M, Volpi M, Sha'afi RI, Hla T. Vascular endothelial cell adherens junction assembly and morphogenesis induced by sphingosine-1-phosphate. Cell. 1999; 99:301–312. [PubMed: 10555146]

Lee MJ, Van Brocklyn JR, Thangada S, Liu CH, Hand AR, Menzeleev R, Spiegel S, Hla T. Sphingosine-1-phosphate as a ligand for the G protein-coupled receptor EDG-1. Science. 1998; 279:1552–1555. [PubMed: 9488656]

Liu Y, Wada R, Yamashita T, Mi Y, Deng CX, Hobson JP, Rosenfeldt HM, Nava VE, Chae SS, Lee MJ, et al. Edg-1, the G protein-coupled receptor for sphingosine-1-phosphate, is essential for vascular maturation. J Clin Invest. 2000; 106:951–961. [PubMed: 11032855]

Montero-Balaguer M, Swirsding K, Orsenigo F, Cotelli F, Mione M, Dejana E. Stable vascular connections and remodeling require full expression of VE-cadherin in zebrafish embryos. PLoS ONE. 2009; 4:e5772. [PubMed: 19503615]

Nicoli S, Standley C, Walker P, Hurlstone A, Fogarty KE, Lawson ND. MicroRNA-mediated integration of haemodynamics and Vegf signalling during angiogenesis. Nature. 2010; 464:1196–1200. [PubMed: 20364122]

Noria S, Cowan DB, Gotlieb AI, Langille BL. Transient and steady-state effects of shear stress on endothelial cell adherens junctions. Circ Res. 1999; 85:504–514. [PubMed: 10488053]

Oo ML, Chang SH, Thangada S, Wu MT, Rezaul K, Blaho V, Hwang SI, Han DK, Hla T. Engagement of S1P1-degradative mechanisms leads to vascular leak in mice. J Clin Invest. 2011; 121:2290–2300. [PubMed: 21555855]

Oo ML, Thangada S, Wu MT, Liu CH, Macdonald TL, Lynch KR, Lin CY, Hla T. Immunosuppressive and anti-angiogenic sphingosine 1-phosphate receptor-1 agonists induce ubipuitinylation and proteasomal degradation of the receptor. Journal of Biological Chemistry. 2007; 282:9082–9089. [PubMed: 17237497]

Paik JH, Chae SS, Lee MJ, Thangada S, Hla T. Sphingosine 1-phosphate-induced endothelial cell migration requires the expression of EDG-1 and EDG-3 receptors and Rho-dependent activation of alpha(v)beta(3)- and beta(1)-containing integrins. Journal of Biological Chemistry. 2001; 276:11830–11837. [PubMed: 11150298]

Paik JH, Skoura A, Chae SS, Cowan AE, Han DK, Proia RL, Hla T. Sphingosine 1-phosphate receptor regulation of N-cadherin mediates vascular stabilization. Genes Dev. 2004; 18:2392–2403. [PubMed: 15371328]

Pitulescu ME, Schmidt I, Benedito R, Adams RH. Inducible gene targeting in the neonatal vasculature and analysis of retinal angiogenesis in mice. Nat Protoc. 2010; 5:1518–1534. [PubMed: 20725067]

Sanchez T, Estrada-Hernandez T, Paik JH, Wu MT, Venkataraman K, Brinkmann V, Claffey K, Hla T. Phosphorylation and action of the immunomodulator FTY720 inhibits vascular endothelial cell growth factor-induced vascular permeability. J Biol Chem. 2003; 278:47281–47290. [PubMed: 12954648]

Sessa WC, Garcia-Cardena G, Liu J, Keh A, Pollock JS, Bradley J, Thiru S, Braverman IM, Desai KM. The Golgi association of endothelial nitric oxide synthase is necessary for the efficient synthesis of nitric oxide. J Biol Chem. 1995; 270:17641–17644. [PubMed: 7543089]

Shiow LR, Rosen DB, Brdickova N, Xu Y, An J, Lanier LL, Cyster JG, Matloubian M. CD69 acts downstream of interferon-alpha/beta to inhibit S1P1 and lymphocyte egress from lymphoid organs. Nature. 2006; 440:540–544. [PubMed: 16525420]

Skoura A, Sanchez T, Claffey K, Mandala SM, Proia RL, Hla T. Essential role of sphingosine 1-phosphate receptor 2 in pathological angiogenesis of the mouse retina. J Clin Invest. 2007; 117:2506–2516. [PubMed: 17710232]

Song JW, Munn LL. Fluid forces control endothelial sprouting. Proc Natl Acad Sci U S A. 2011; 108:15342–15347. [PubMed: 21876168]

Stenzel D, Franco CA, Estrach S, Mettouchi A, Sauvaget D, Rosewell I, Schertel A, Armer H, Domogatskaya A, Rodin S, et al. Endothelial basement membrane limits tip cell formation by inducing Dll4/Notch signalling in vivo. EMBO Rep. 2011; 12:1135–1143. [PubMed: 21979816]

Suchting S, Freitas C, le Noble F, Benedito R, Breant C, Duarte A, Eichmann A. The Notch ligand Delta-like 4 negatively regulates endothelial tip cell formation and vessel branching. Proc Natl Acad Sci U S A. 2007; 104:3225–3230. [PubMed: 17296941]

Thibeault S, Rautureau Y, Oubaha M, Faubert D, Wilkes BC, Delisle C, Gratton JP. S-nitrosylation of beta-catenin by eNOS-derived NO promotes VEGF-induced endothelial cell permeability. Mol Cell. 2010; 39:468–476. [PubMed: 20705246]

Tzima E, Irani-Tehrani M, Kiosses WB, Dejana E, Schultz DA, Engelhardt B, Cao G, DeLisser H, Schwartz MA. A mechanosensory complex that mediates the endothelial cell response to fluid shear stress. Nature. 2005; 437:426–431. [PubMed: 16163360]

Tzima E, Kiosses WB, del Pozo MA, Schwartz MA. Localized cdc42 activation, detected using a novel assay, mediates microtubule organizing center positioning in endothelial cells in response to fluid shear stress. J Biol Chem. 2003; 278:31020–31023. [PubMed: 12754216]

Venkataraman K, Lee YM, Michaud J, Thangada S, Ai Y, Bonkovsky HL, Parikh NS, Habrukowich C, Hla T. Vascular endothelium as a contributor of plasma sphingosine 1-phosphate. Circ Res. 2008; 102:669–676. [PubMed: 18258856]

Wadhwa S, Godwin SL, Peterson DR, Epstein MA, Raisz LG, Pilbeam CC. Fluid flow induction of cyclo-oxygenase 2 gene expression in osteoblasts is dependent on an extracellular signal-regulated kinase signaling pathway. J Bone Miner Res. 2002; 17:266–274. [PubMed: 11811557]

Wang DA, Lorincz Z, Bautista DL, Liliom K, Tigyi G, Parrill AL. A single amino acid determines lysophospholipid specificity of the S1P1 (EDG1) and LPA1 (EDG2) phospholipid growth factor receptors. J Biol Chem. 2001; 276:49213–49220. [PubMed: 11604399]

Zeeb M, Strilic B, Lammert E. Resolving cell-cell junctions: lumen formation in blood vessels. Curr Opin Cell Biol. 2010; 22:626–632. [PubMed: 20678912]

Highlights

$S1P_1$ is expressed in nascent vascular networks and suppresses hypersprouting

Endothelial $S1P_1$ promotes barrier function and flow in vascular networks

Flow-mediated signaling and morphological changes require $S1P_1$

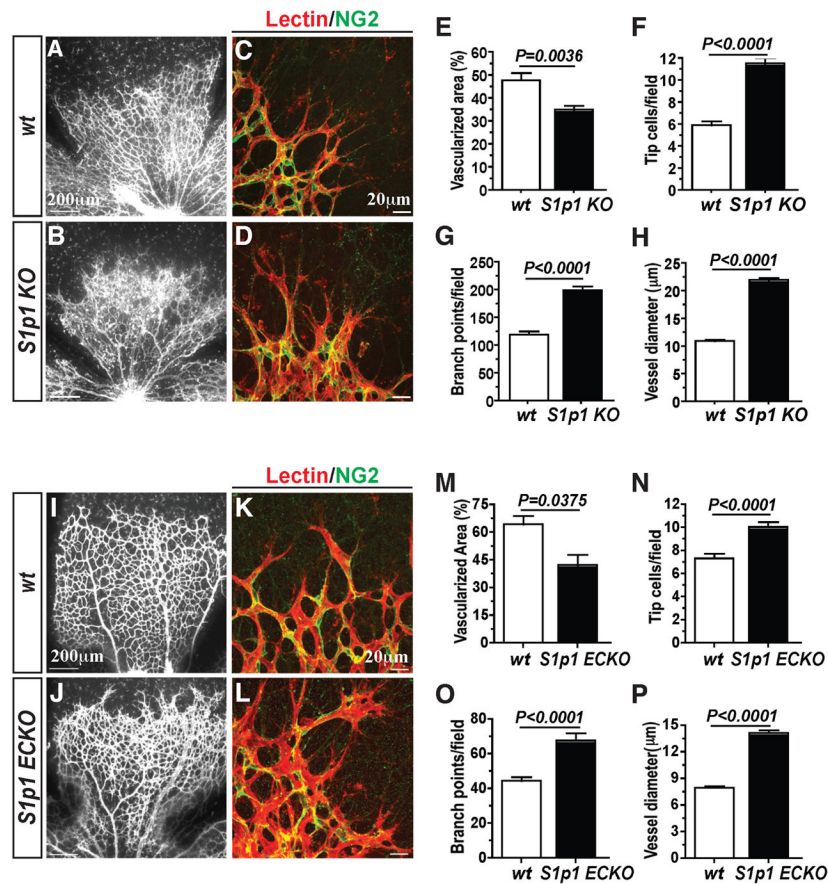Flow activates $S1P_1$ receptor in a ligand-independent manner

Figure 1. Endothelial S1P$_1$ regulates retinal vascular development
(A–D) Retinas from postnatal day 4 (P4) *S1p1 KO* animals [WT (n=6) and *S1p1 KO* (n=7)] were stained in lectin to visualize retinal vasculature. Vascularization (E), tip cell numbers (F), branch points (G), and vessel diameter (H) were quantitated as described in Experimental Procedures. (I–L) EC-specific loss of S1P$_1$ (*S1p1 ECKO*) resulted in retinal hypersprouting. Reduced vascularization (M), increased tip cell numbers (N), reduced branch points (O), and increased vessel diameter (P) were also observed in *S1p1 ECKO* animals [WT (n=3) and *S1p1 ECKO* (n=6)]. See also Figures S1 and S2. All values are mean ± SEM.
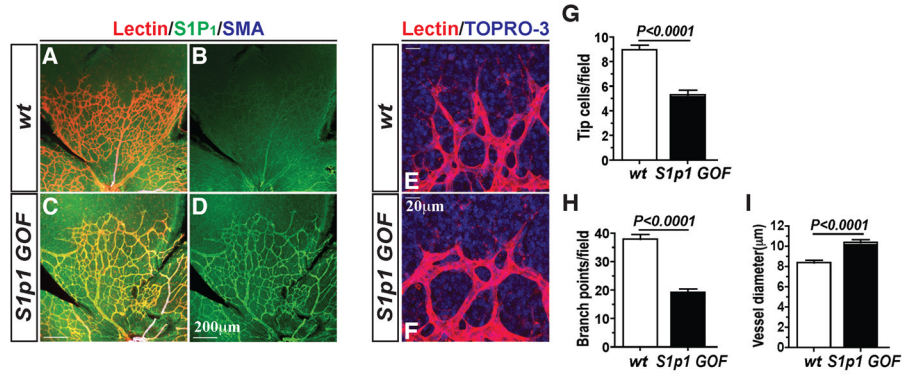
Figure 2. S1P$_1$ overexpression (*S1p1 GOF*) suppresses sprouting angiogenesis
(A–F) Retinal vascular plexus formation in *S1p1 GOF* (P5) mice. S1P$_1$ immunostaining is shown in B and D. Note that the vessel density and the number of tip cells were markedly reduced upon S1P$_1$ overexpression. (E and F) High power images of the growing vessels at the tip. Quantification results from *S1p1 GOF* mouse retinas displayed reduced sprouting of tip cells (G), reduced branch points (H) and increased dilation of the vessels (I) [WT (n=4) and *S1p1 GOF* (n=5)]. See also Figure S1. All values are mean ± SEM.
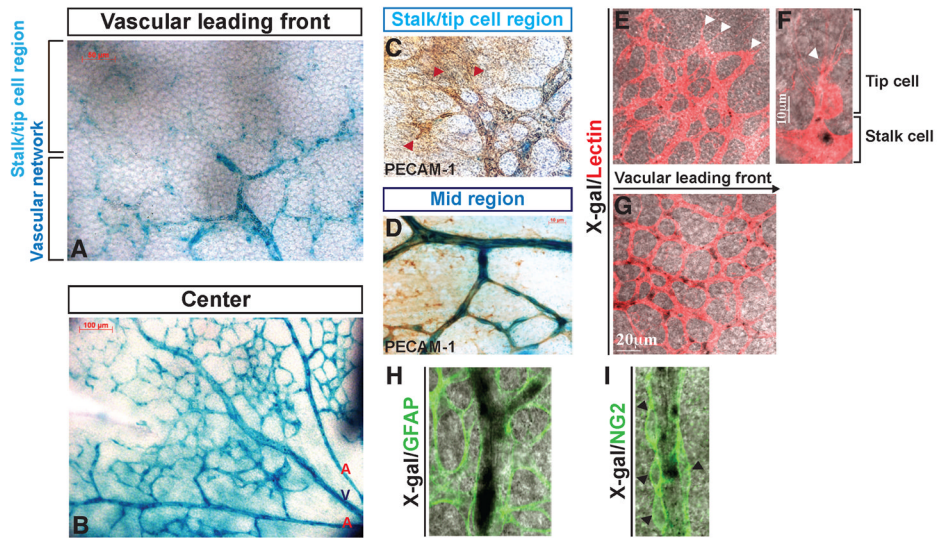
Figure 3. Gradient of S1P₁ expression in the developing retinal vasculature

(A and B) The expression of the *S1pr1* locus in the retinal vasculature was examined by X-gal staining using P4 *S1pr1^LacZ/+* mice (shown in blue), in combination with PECAM-1 (C and D), lectin (E–G), GFAP (H) or NG2 (I) co-staining. Note that high LacZ activity was detected in mature vascular ECs compared to the vascular leading front, and that LacZ expression is restricted to endothelium. Red and white arrowheads indicate tip cells (C, E, and F), and black arrowheads denote NG2⁺ cells (I). See also Figure S3.
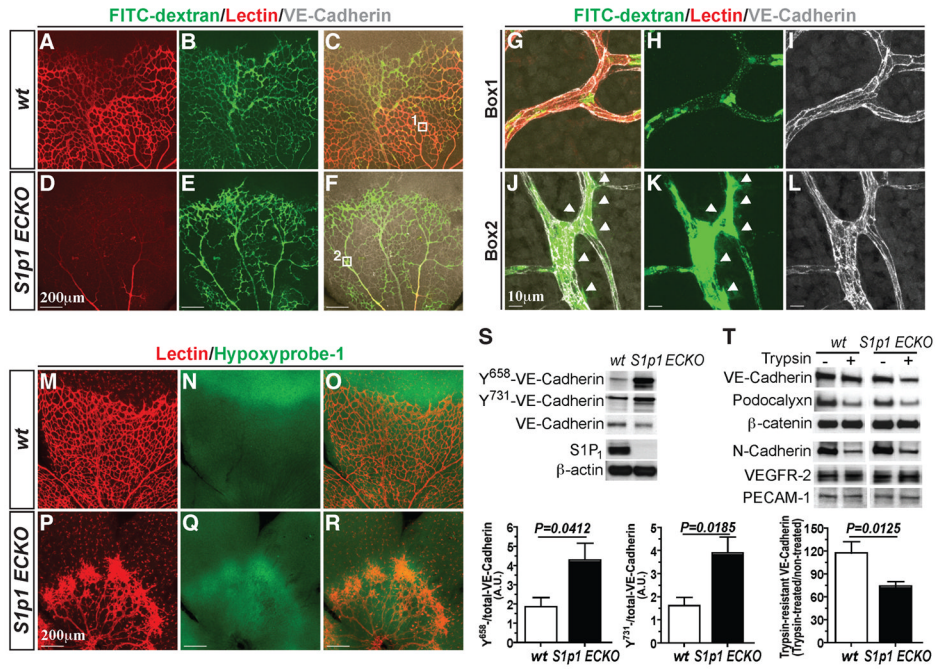
Figure 4. S1P$_1$ is critical for stabilization of the flow-competent vessels

(A–J) Retinas from WT and *S1p1 ECKO* mice were imaged after intracardiac injection of FITC-Dextran (M$_r$~ 2,000 kDa) and lectin. High power images of the WT (Box1, G–I) and *S1p1 ECKO* (Box2, J–L) retinas. Arrowheads indicate sites of vascular leakage. (M–R) Retinal hypoxia was visualized by Hypoxyprobe-1 staining as described in Experimental Procedures. (S) Total lung lysates from WT and *S1P1 ECKO* animals were analyzed for Y^{658}-, and Y^{731}-VE-cadherin levels by immunoblots [WT (n=5) and *S1p1 ECKO* (n=5)]. (T) Retina explants were treated with 0.05 % trypsin for 60 min and total protein extracts were analyzed for EC markers. Note that VE-cadherin is more sensitive to trypsin in *S1p1 ECKO* retinas [WT (n=3) and *S1p1 ECKO* (n=6)]. See also Figure S4. All values are mean ± SEM.
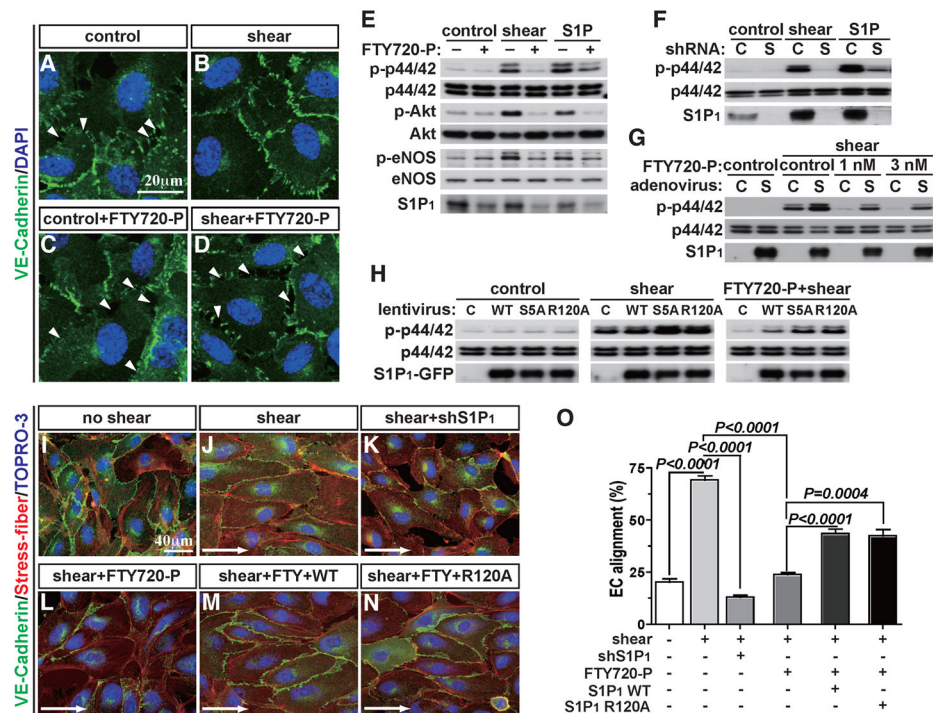
Figure 5. S1P₁ is required for shear stress-induced signaling in EC *in vitro*

(A–D) HUVEC were pretreated with FTY720-P, and laminar shear (8 dynes/cm²) was applied for 1 hr. Adherens junction formation was visualized by VE-cadherin immunofluorescence staining. Arrowheads indicate intercellular gaps (E–G) ERK, Akt and eNOS activation were examined 10 min after laminar shear application in the presence or the absence of FTY720-P (E), shRNA for S1P₁ (F), FTY720-P with adenoviral overexpression of S1P₁ (G). (H) Short-term laminar shear was applied to WT, S5A, or R120A mutants and immunoblots for ERK activation were carried out. (I–N) shRNA for S1P₁-treated cells, FTY720-P-treated WT or R120A mutant cells underwent long-term laminar shear (12 hr), and EC alignment was examined. Percentage of the aligned cell numbers over the total cell numbers were quantified as described in Experimental Procedures (O). See also Figure S5. All values are mean ± SD.

Figure 6. *In vivo* **requirement for S1P₁ in shear stress signaling**

(A–D) Expression of S1P₁ and VE-cadherin in areas of laminar (descending) and turbulent shear (lesser curvature) in the aorta. Sections of the aorta were dissected and stained for S1P₁ and VE-cadherin (A and B) or EEA-1 (C and D) in *en face* preparations. (E–J) Sections of the aorta were stained for total-eNOS (E and F) and phospho-eNOS (G and H). Quantification of phospho-(I) and total-eNOS (J) levels in WT ad *S1p1 ECKO* descending aortas is shown [WT (n=4) and *S1p1 ECKO* (n=4)]. (K and L) Retinal tissues from WT and *S1p1 ECKO* (P5) were analyzed for phospho-eNOS and total-eNOS levels by immunoblots [WT (n=5) and *S1p1 ECKO* (n=4)]. (M and N) Quantification of the morphological changes observed in the descending aortic region from WT and *S1p1 ECKO* mice is shown. [WT (n=4) and *S1p1 ECKO* (n=4)]. All values are mean ± SEM.